Defence Science Journal, Vol. 75, No. 1, January 2025, pp. 44-51, DOI : 10.14429/dsj.20551

An Application of Machine Learning in Empirical and Variational Mode Decomposition with SVM Classifier to Enhance Diagnostic Accuracy for Disease Detection in Soldier`s Eyes

Pooja Manghnani* and Asmita A. Moghe

University Institute of Technology, Rajiv Gandhi Proudyogiki Vishwavidyalaya, Bhopal - 462 033, India
**E-mail: poojam2673@gmail.com*

ABSTRACT

Soldiers rely heavily on their vision, which is crucial not only for daily activities but also for the effective operation of defense systems, weaponry, and other military applications. However, various eye disorders, such as those related to increased intra-ocular pressure, can lead to irreversible vision loss, severely impacting a soldier's operational capabilities. While extensive research has been conducted on detecting such ocular conditions, there remains a critical need for more accurate diagnostic methods to ensure early detection and treatment. In this study, we propose a novel approach combining Empirical Mode Decomposition (EMD) and Variational Mode Decomposition (VMD) for enhanced detection of eye disorders from retinal fundus images. The proposed method includes a comprehensive preprocessing phase, followed by decomposition using EMD and VMD techniques. The decomposed images undergo feature extraction through feature combination, with subsequent normalization and selection using z-score and the Relief method, respectively. Classification is performed using Support Vector Machines (SVM) with various kernels, including cubic, Gaussian, linear, and quadratic. The results demonstrate that the proposed method achieves high accuracy, with SVM kernel functions yielding accuracies of 98.30 %, 96.59 %, 96.59 %, and 97.87 % for 10-fold cross-validation, respectively. Additionally, the evaluation metrics, including sensitivity and specificity, indicate superior performance compared to state-of-the-art methods for similar datasets. This advanced diagnostic approach offers significant improvements in detecting eye disorders, which could be crucial in defense applications. Early and accurate diagnosis by military ophthalmologists can lead to better decision-making and timely interventions, ultimately preserving the vision and effectiveness of soldiers in the war.

Keywords: Eye disorders; Defense applications; Empirical Mode Decomposition (EMD); Support Vector Machines (SVM); Retinal fundus images; Early diagnosis

NOMENCLATURE

EMD : Empirical mode decomposition
VMD : Variational mode decomposition
SVM : Support vector machines
PCA : Principal component analysis
OHAWT: Optimal hyper analytic wavelets transform
CVMD : Compact variational mode decomposition
IMFs : Intrinsic mode functions
BDIMFs: Bidimensional intrinsic mode functions

1. INTRODUCTION

The human eye is an essential part of the body, especially in defense, where a soldier's readiness and effectiveness on the battlefield depend heavily on sharp vision. In the chaos of war, with guns firing, smoke filling the air, and explosions lighting up the sky, the ability to see clearly can mean the difference between life and death. However, certain ocular ailments, like those caused by increased intra-ocular pressure, can lead to devastating consequences such as permanent vision loss or blindness. These conditions, which develop insidiously, gradually damage the optic nerves within the eye, reducing a soldier's capability to operate in environments filled with flames, explosions, and other hazards. The World Health Organization has identified this condition as the second leading cause of vision loss worldwide, with the number of affected individuals expected to rise to 111.8 million by the year 2040[1-5].

Received : 13 September 2024, Revised : 22 October 2024
Accepted : 06 November 2024, Online published : 10 January 2025

1.1 Literature Review

Various works have been reported for the glaucoma detection in the last decade. Bock*, et. al.*[1] implemented Principal Component Analysis (PCA) on a transformed images followed by classification using a Support Vector Machine (SVM). Raja[6]*, et. al.* proposed automated glaucoma detection approach using Optimal Hyper Analytic Wavelets Transform (OHAWT). Maheshwari[7]*, et. al.* proposed variational mode decomposition (VMD) method-based glaucoma detection. Kirar[8]*, et. al.* proposed Discrete Wavelet Transform (DWT) and empirical wavelet transform (EWT) methods-based glaucoma detection. Kirar[9]*, et. al.* designed an automated glaucoma detection method using Compact Variational Mode Decomposition (CVMD). Agrawal[10]*, et. al.* proposed Quasi-Bivariate Variational Mode Decomposition (QB-VMD) method-based glaucoma detection using. Further, Kirar[12]*, et. al.* proposed

new approach using DWT image channels. Diaz-Pinto[13], *et. al.* proposed and developed new ACRIMA image dataset with 705 images for glaucoma detection using Convolutional Neural Network (CNNs). Further, various works[10-20] have been reported on this recent popular ACRIMA dataset[13]. Serte, *et. al.*[14] implemented his work on ACRIMA dataset for glaucoma detection using Deep Learning (DL). Claro[15], *et. al.* developed new approach using Transfer Learning (TL), hybrid feature and Random Forest (RF) classifier. Liu[17], *et. al.* added deep NN for feature extraction and classification. Elangovan[18], *et. al.* modeled a standard CNN using softmax classifier. Kirar[19], *et. al.* in new research work, implemented QB-VMD in two stages with SVM. Galarraga[20], *et. al.* successfully implemented image processing techniques for glaucoma detection. Devi[21], *et. al.* also implemented successfully various texture-based method for feature extraction and classification. Manghnani[22], *et. al.* proposed an improved method using bidimensional EMD (BD-EMD) for glaucoma detection. Devecioglu[23], *et. al.* developed a compact Self-Organized Operational Neural Networks method for glaucoma detection.

Some most recently published articles include, Singh[24], *et. al.* proposed a multimodality-based approach for efficient glaucoma prediction. Early fusion and late fusion both were implemented in this work. Machine Learning and Deep learning were implemented using feature level fusion and image level fusion respectively. Approach was tested on three benchmark datasets and four combinations of these datasets. Classification accuracy up to 92.14 % was achieved through this approach using ACRIMA dataset. Sonti[25], *et. al.* implemented QB-VMD with shape and texture-based features for better performances. Other works also proposed enhanced glaucoma detection from fundus images[26-28]

1.2 Limitations in Existing Research Work

Research work published for glaucoma detection[1-7,25-35] reported less accuracy. It may be due to having some demerit or due to limitation of methods used or have not utilized the contribution of all components. Methods used based on DWT[7-9] have interference with little resolution. Methods used based on EWT[5] suffer from redundancy. Methods used based on EMD[17] and VMD[7-24] the EMD have problem of boundary distortion which is overcome by use of VMD based methods. VMD based methods are better. Further, VMD is also limited to large and varied data set. There is lack of contribution of all color components in the methods used based on ML DL[36-45] and DL[13-18, 46-58] However, there is a scope to develop a model for improved glaucoma detection by combining EMD and VMD based methods.

1.3 Contributions in the Proposed Work

During image capturing, if precautions are not taken then the image quality may degrade by the addition of some nearby noise and artefacts. Continuing with the research work[22], we further propose a combination of EMD and VMD based methods for improved glaucoma detection from retinal fundus images. This paper includes the following contributions:

- It involves the study of latest research work for glaucoma detection
- Images are subjected to preprocessing using rescaling and decomposition into its gray scale, green, red and blue components
- All components are subjected to EMD and VMD methods for decomposition into their corresponding small, moderate and high frequency components
- Further, extracted and selected features are classified with SVM–based kernels, like Linear, Quadratic, Cubic, and Gaussian. SVM with Cubic kernel gives the best performance.

2. PROPOSED RESEARCH WORK

This section describes the proposed research work in detail as shown in Fig.1 First of all, ACRIMA images are rescaled and subjected to decomposition to gray scale, green, red and blue components. Then each component is subjected to EMD and VMD based methods separately. Then all the decomposed frequency components, intrinsic mode functions (IMFs) are subjected to features extraction methods. Finally, obtained features are combined and subjected to z-score normalization and relief features selection followed by classification using support vector machines (SVM) with its different kernels like linear, quadratic, cubic, and gaussian. Performance metrics are evaluated and compared with state of art work.

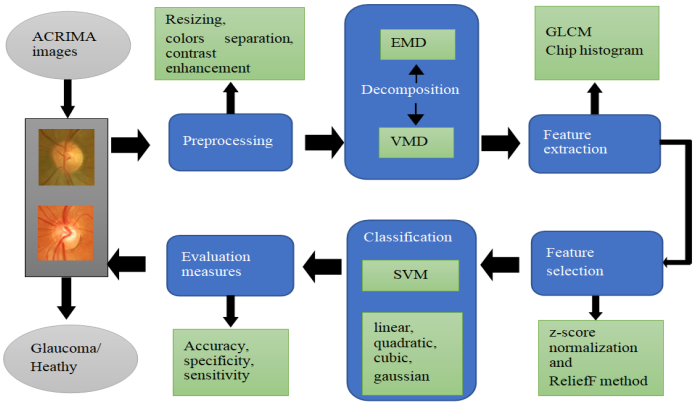

Figure 1. Block diagram of the proposed work.

2.1 ACRIMA Images Data Set

This dataset includes a total 705 images (396 Glaucoma+ 309 Healthy) and available in .jpg image format publically[13]. ACRIMA images are captured with a field of view of 35° and pixel values vary from 178×178 to 1420×1420.

2.2 Pre-Processing

Image capturing process may add some unwanted noised and artefacts, which is responsible for the lower image quality and hence somewhat reduced performance. To enhance the performance rescaling and contrast enhancement are applied to the images[1]. This work includes rescaling and decomposition into its gray scale, green, red and blue components followed by equalisation and filtering[29]. Outputs of all steps involved in preprocessing of glaucoma and healthy images are shown in Fig. 2 & 3.

2.3 Empirical Mode Decomposition

This section explains the empirical mode decomposition

(EMD). It is adaptive in nature. Its bi-dimensional form (BDEMD) decomposes input image into three frequency components, Intrinsic Mode Functions (IMFs) and one residue. It has the advantage to decompose the image into small, moderate & high frequency components, bidimensional IMFs (BDIMFs)[31] The decomposition of image I(x,y) using BDEMD is carried out as follows:

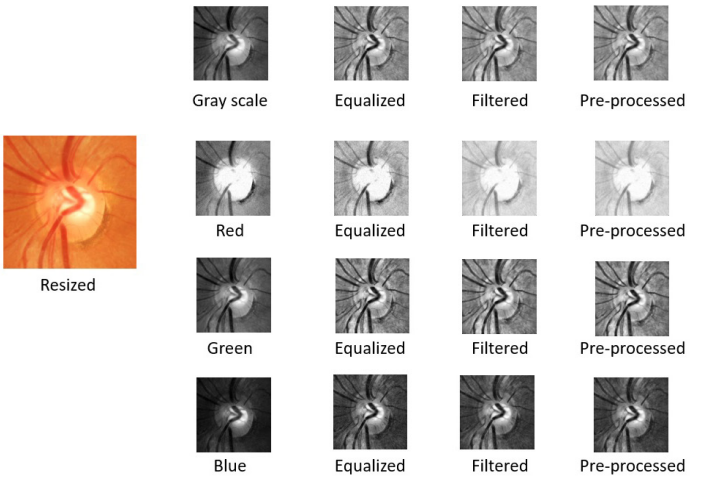

Figure 2. Outputs of all steps involved in preprocessing of glaucoma image.

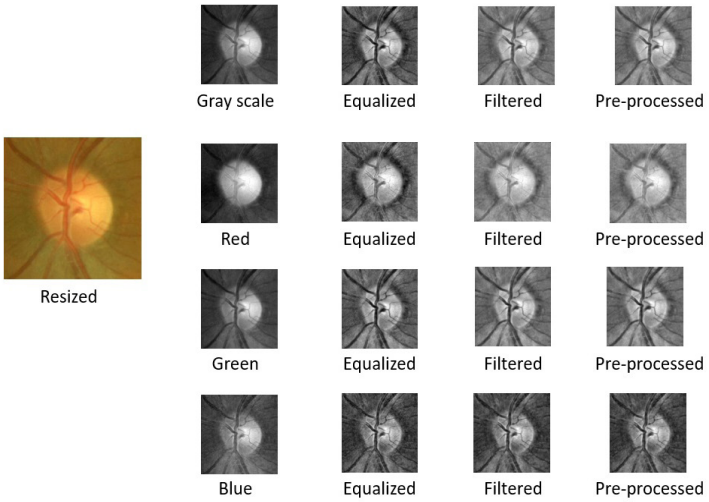

Figure 3. Outputs of all steps involved in preprocessing of healthy image.

- Calculation of maxima and minima of I(x,y).
- Calculation of upper and lower envelope of I(x,y).
- Calculation average envelope by adding upper and lower envelope of I(x,y) and dividing by 2.
- Subtraction of the average envelope from input image. Then we check the result for stopping criterion. If a match occurs implies it is a BDIMF and we move ahead to the next step (v) Else are go back and start from step(i)-(iii). Taking the result as input, we find new BDIMF.
- Calculate remaining BDIMFs, taking result of step (iv) as input and repeat steps (i-iv).

Finally, BDEMD decomposes image as a sum of BDIMFs (s=1 to 3) and one residue as given in Eqn. (1). Where s is from 1 to 3.

$$I(x,y)=\sum_{s=1}^{S} BDIMF_s(x,y)+Res(x,y) \tag{1}$$

2.4 Variational Mode Decomposition

This section explains the variational mode decomposition (VMD). It is non-stationary and fully adaptive in nature. Its two-dimensional form (2DVMD) decomposes input image into five frequency components, intrinsic mode functions (IMFs). It is more advantageous than conventional methods to decompose the image into small, moderate & high frequency components (VMDIMFs) because it has no mode mixing problems. VMDIMFs are band limited and centered around a specific frequency, which are calculated using Eqn. (2-6) as follows[32]:

Variational problem for VMD

$$\min_{z_n \omega_n}\left\{\sum_n \left\| dt\left[\left(\delta(t)+\frac{i}{\pi t}\right)* z_n(t)\right]e^{-i\omega_t}\right\|^2\right\} \tag{2}$$

Such that

$$\sum_n z_n = S \tag{3}$$

The above Eqn. is rewritten as:

$$\mathcal{L}(Z_n,W_n,\beta)=\alpha\sum_n\left\|dt\left[\left(\delta(t)+\frac{i}{\pi t}\right)*Z_n(t)\right]e^{-i\omega_n t}\right\|_2^2 + \left\|s(t)-\sum_n Z_n(t)\right\|_2^2+\left\langle\beta(t),s(t)-\sum_n u_n(t)\right\rangle \tag{4}$$

The estimated n^{th} VMDIMFs are given as:

$$\hat{z}_n^{m+1}(\omega)=\frac{\hat{S}(\omega)-\sum_{j\neq n}\hat{y}_j(\omega)+\frac{\hat{\beta}(\omega)}{2}}{1+2\alpha(\omega-\omega_n)^2} \tag{5}$$

The center frequency can be expressed as:

$$\omega_n^{m+1}=\frac{\int_0^\infty \omega\left|\hat{z}_n(\omega)\right|^2 d\omega}{\int_0^\infty\left|\hat{z}_n(\omega)\right|^2 d\omega} \tag{6}$$

where, S = signal, α =balancing parameter, z_n=VMDIMFs, and ω_n=center frequency of n^{th} VMD component.

2.5 Feature Extraction and Selection

Total 4-GLCM (Gray-Level Co-Occurrence Matrix) and 6-chip histogram features[34] as listed in Table1 are extracted from all decomposed components. We have extracted 40 features from EMDIMFs and 40 features from VMDIMFs i.e. a total of 80 features have been extracted.

Table 1. Features extracted from various components

Features	No of features	Name of features
GLCM	4	Contrast Correlation Energy Homogeneity
Chip histogram features	6	Energy Mean Entropy Variance Kurtosis Skewness

These 80 features are subjected to z-score normalisation[22] and ReliefF features selection method[35] for obtaining important features only. This step is used to increase the performance of SVM classifier. A z-score normalization ($\hat{F}$) is calculated using Eqn. (7).

$$\hat{F} = \frac{F - m(F)}{sd(F)} \tag{7}$$

where, *sd*=standard deviation, *m*=mean, *F*= extracted features data.

2.6 Classification

Widely used classifier in the medical image field is support vector machine[36,59-62]. This research work is implemented using SVM with its kernels like Cubic, Gaussian, Linear, Quadratic and hence named as C-SVM, G-SVM, L-SVM, and Q-SVM. The SVM and performance evaluation measures[30-71] include accuracy (Acc), sensitivity (Sen), and specificity (Spe), which are calculated using Eqn. (8-10).

$$Acc = \frac{TP + TN}{TP + TN + FP + FN} \times 100 \tag{8}$$

$$Sen = \frac{TP}{TP + FN} \times 10 \tag{9}$$

$$Spe = \frac{TN}{TN + FP} \times 100 \tag{10}$$

where,
TP=True+Positive. TN=True+Negative, FP=False+Positive and FN=False+Negative.

3. EXPERIMENTAL RESULTS

In this paper a combination of EMD and VMD based methods for improved glaucoma detection is implemented on ACRIMA[13] image dataset. Two input images of glaucoma (Im638_g_ACRIMA.jpeg) and healthy (Im056_ACRIMA.jpeg) are given in Fig. 4. After applying preprocessing and decomposition methods, separately. We obtained various frequency components (EMD-imfs and VMD-imfs) from low to moderate, and moderate to high using EMD[69-76] and VMD[52-68] as shown in Fig. 4. The evaluated matrices like accuracy, sensitivity, and specificity of proposed work using 10-fold cross validation are presented in Table 2. The achieved accuracy using SVM with its kernel functions like cubic, gaussian, linear, quadratic is 98.30 %, 96.59 %, 96.59 %, and 97.87 %, respectively Fig. 4.

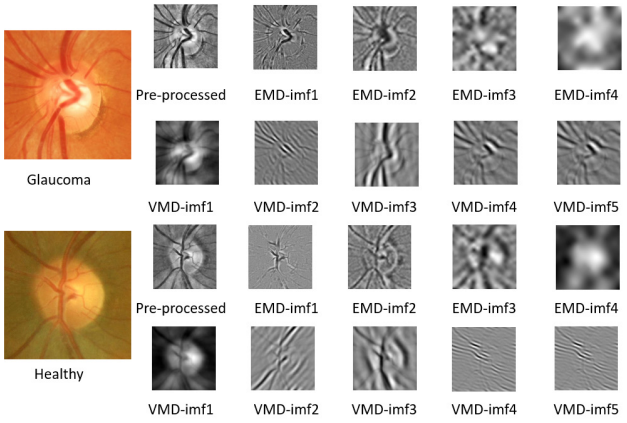

Figure 4. Input sample images along with sample images along with preprocessed and EMD-imfs and VMD-imfs.

Table 2. Performance for the proposed work after 3, 5, & 10 fold cross validation with different kernel

k-FCV	SVM Kernels	Acc (%)	Sen (%)	Spe (%)
3	Linear	95.74	97.47	93.51
	Quadratic	97.3	98.48	95.78
	Cubic	97.59	98.48	96.43
	Gaussian	95.86	99.74	90.91
5	Linear	96.16	97.73	94.16
	Quadratic	97.3	98.23	96.1
	Cubic	97.87	98.74	96.75
	Gaussian	96.31	99.24	92.53
10	Linear	96.59	98.23	94.48
	Quadratic	97.87	98.74	96.75
	Cubic	98.3	98.48	98.05
	Gaussian	96.59	99.75	92.53

In Fig. 5, we have plotted a curve for performance (in percentage) of proposed research work using 4 types of SVM-kernel for 2-to-13-fold cross validation. In Fig. 5, we obtained better accuracy using cubic and quadratic kernels with SVM for 10-fold cross validation. However, C-SVM achieved highest accuracy with better sensitivity and specificity. This showed that 10-fold is better for C-SVM.

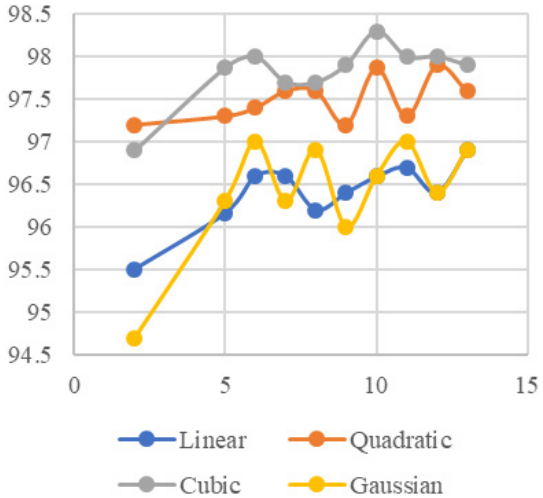

Figure 5. Plot for accuracy (in %) versus SVM-Kernels for 2-to-13-fold cross validation.

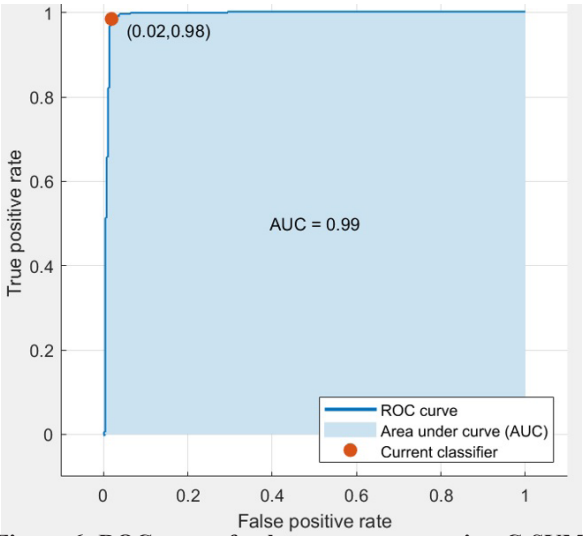

Figure 6. ROC curve foe better accuracy using C-SVM.

Further, we have also plotted a ROC curve for better accuracy using C-SVM in Fig. 6 for 10-fold cross validation.

4. COMPARATIVE ANALYSIS OF PROPOSED AND EXISTING RESEARCH WORK

This section presents an experimental comparison of proposed research work and recent state-of-the-art method for glaucoma detection.

Table 3. Comparison of methods (ACRIMA dataset)

Research work	Performances (%)		
Author/ref./year	Acc.	Sen.	Spe.
Pinto, *et. al.*[13]/2019	70.21	68.93	70.2
Serte, *et. al.*[14]/2019	65	NR	87
Claro et. al al.[15]/2019	95.31	NR	NR
Liu, *et. al.*[17]/2020	85.1	85.4	84.3
Elangovan, *et. al.*[18]/2020	96.64	96.07	97.39
Kirar, *et. al.*[19]/2021	92.06	91.42	92.89
Galarraga, *et. al.*[20]/2021	94.61	94.57	92.5
Devi, *et. al.*[21]/2021	95	94.11	95.91
Manghnani, *et. al.*[22]/2021	97.02	98.23	95.46
Devecioglu, *et. al.*[23]/2022	91.8	93.6	88.8
Singh, *et. al.*[24]/2022	92.14	92	90
Sonti, *et. al.*[25]/2022	96.7	98.32	94.62
Bouris, *et. al.*[71]/2024	92	98	80
Wiharto, *et. al.*[72]/2024	97.99	97.99	97.71
Manghnani, *et. al.*[73]/2024	91.6	96.3	96.7
Proposed work	98.29	98.48	98.05

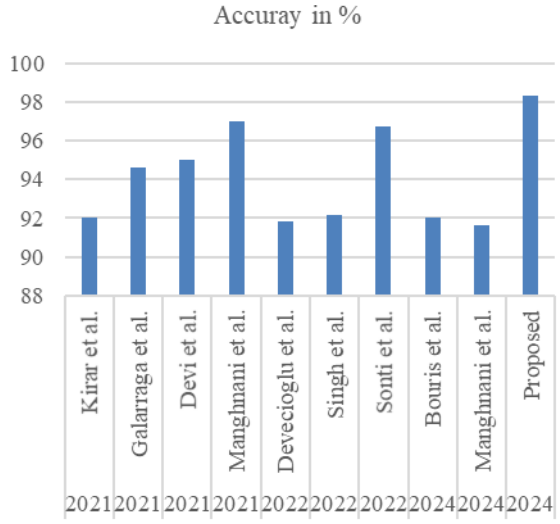

Figure 7. Accuracy comparison for recent methods only (in %).

Various work has been studied in the literature survey part; here we compared some research work implemented on ACRIMA dataset[13]. Pinto[13], *et. al.*, Serte[14], *et. al.*, Claro[15], *et. al.*, Liu[17], *et. al.*, Elangovan[18], *et. al.*, Kirar[19], *et. al.*, Galarraga[20], *et. al.*, Devi[21], *et. al.*, Manghnani[22], *et. al.*, Devecioglu[23], *et. al.*, and Singh[24], *et. al.*, Sonti[25], *et. al.* Compared research work[13-25] reported comparatively less accuracy. It may be due to limitation of methods used or have not utilised the contribution of all components.

Proposed research work achieved better results. We have obtained highest accuracy, which is 98.30 %, using C-SVM. The achieved accuracy using SVM with its kernel functions like cubic, gaussian, linear, quadratic is 98.30 %, 96.59 %, 96.59 %, and 97.87 %, respectively. The performances comparison of this work and recent published work has been given in Table 3 and plotted in Fig. 7.

5. CONCLUSIONS AND FUTURE WORK

This research presents a combined Empirical Mode Decomposition (EMD) and Variational Mode Decomposition (VMD) approach for enhanced detection of ocular diseases from retinal fundus images. In defense scenarios, where soldiers, fighter pilots, tank operators, and infantry must maintain peak visual performance amidst the chaos of war-guns firing, rockets launching, cannons booming, and explosions lighting up the battlefield-accurate and early diagnosis of eye conditions is crucial. By preprocessing and decomposing all color components using EMD and VMD into EMD-imfs and VMD-imfs, the accuracy of detecting these conditions has been significantly improved. The C-SVM classifier achieved the highest accuracy of 98.30 %, demonstrating superior performance on the ACRIMA image dataset with 10-fold cross-validation. The achieved accuracies using SVM with cubic, Gaussian, linear, and quadratic kernels were 98.30 %, 96.59 %, 96.59 %, and 97.87 %, respectively. When compared to other methods, our proposed approach outperforms state-of-the-art techniques, leading to better results for detecting ocular diseases.

This method, with its improved accuracy, can assist military ophthalmologists in making better decisions for the diagnosis of eye conditions in defense applications. The ability to diagnose eye diseases early can help maintain the readiness and effectiveness of soldiers, pilots, and other defense personnel in high-stress environments filled with flames, explosions, and smoke. As future work, this approach could be extended to include deep learning features for detecting not only ocular diseases but also other conditions such as diabetes and retinopathy, further advancing its application in defense contexts.

REFERENCES

1. Sharma, A.; Patra, G.K. & Naidu, V.P.S. Machine learning based bearing fault classification using higher order spectral analysis. *Def. Sci. J.*, 2024, **74**, 505-516. doi:10.14429/dsj.74.19307.
2. Priyadarshini, S.; Gourab, M.K.; Mandal, U. & Roy, A. A comparative study on various flight termination system technologies. *Def. Sci. J.*, 2023, **73**, 351-361. doi:10.14429/dsj.73.18334.
3. S, G.; T, D. & Haldorai, A. A supervised machine learning model for tool condition monitoring in smart manufacturing. *Def. Sci. J.*, 2022, **72**, 712-720. doi:10.14429/dsj.72.17533.
4. Bock, R.; Meier, J.; Nyúl, L.G.; Hornegger, J. & Michelson, G. Glaucoma risk index: automated glaucoma detection from color fundus images. *Med. Image Anal.*, 2010, **14**(3), 471-481. doi:10.1016/j.media.2009.12.006.

5. Tham, Y.C.; Li, X.; Wong, T.Y.; Quigley, H.A.; Aung, T. & Cheng, C.Y. Global prevalence of glaucoma and projections of glaucoma burden through 2040: A systematic review and meta-analysis. *Ophthalmol.,* 2014, **121**(11), 2081-2090. doi:10.1016/j.ophtha.2014.05.013.
6. Raja, C. & Gangatharan, N. Optimal hyper analytic wavelet transform for glaucoma detection in fundal retinal images. *J. Electr. Eng. Technol*., 2015, **10**(4), 1899-1909. doi:10.5370/jeet.2015.10.4.1899.
7. Maheshwari, S.; Pachori, R.B.; Kanhangad, V.; Bhandary, S.V. & Acharya, U.R. Iterative variational mode decomposition based automated detection of glaucoma using fundus images. *Comput. Biol. Med*., 2017, **88**, 142-149. doi:10.1016/j.compbiomed.2017.06.017.
8. Kirar, B.S. & Agrawal, D.K. Computer aided diagnosis of glaucoma using discrete and empirical wavelet transform from fundus images. *IET Image Process*., 2019, **13**(1), 73–82. doi:10.1049/iet-ipr.2018.5297.
9. Kirar, B. & Agrawal, D. Current research on glaucoma detection using compact variational mode decomposition from fundus images. *Int. J. Intell. Eng. Syst*., 2019, **12**(3), 1–10. doi:10.22266/ijies2019.0630.01.
10. Agrawal, D.K.; Kirar, B.S. & Pachori, R.B. Automated glaucoma detection using quasi-bivariate variational mode decomposition from fundus images. *IET Image Process*., 2019, **13**(13), 2401–2408. doi:10.1049/iet-ipr.2019.0036.
11. Rathore, N. & Chana, I. Job migration with fault tolerance based QoS scheduling using hash table functionality in social grid computing. *J. Intell. Fuzzy Syst*., 2014, **27**(6), 2821–2833. doi:10.3233/ifs-141243.
12. Kirar, B.S.; Agrawal, D.K. & Kirar, S. Glaucoma detection using image channels and discrete wavelet transform. *IETE J.* Res., 2022, **68**(6), 4421–4428. doi:10.1080/03772063.2020.1795934.
13. Diaz-Pinto, A.; Morales, S.; Naranjo, V.; Köhler, T.; Mossi, J.M. & Navea, A. CNNs for automatic glaucoma assessment using fundus images: an extensive validation. *Biomed. Eng. Online*., 2019, **18,** 1-19. doi:10.1186/s12938-019-0649-y.
14. Serte, S. & Serener, A. A generalized deep learning model for glaucoma detection. *In* 3rd International Symposium on Multidisciplinary Studies and Innovative Technologies (ISMSIT), 2019, 1-15. doi:10.1109/ismsit.2019.8932753.
15. Claro, M.; Veras, R.; Santana, A.; Araújo, F.; Silva, R.; Almeida, J. & Leite, D. An hybrid feature space from texture information and transfer learning for glaucoma classification. *J. Visual. Commun. Image Represent*., 2019, **64**, 102597. doi:10.1016/j.jvcir.2019.102597.
16. Chana, I. A sender initiate based hierarchical load balancing technique for grid using variable threshold value. 2013, 1-6. doi:10.1109/ispcc.2013.6663440.
17. Liu, H.; Zhang, N.; Jin, S.; Xu, D. & Gao, W. Small sample color fundus image quality assessment based on gcforest. *Multimed., Tools Appl*. 2021, **80**, 17441–17459. doi:10.1007/s11042-020-09362-y.
18. Elangovan, P. & Nath, M.K. Glaucoma assessment from color fundus images using convolutional neural network. *Int. J. Imaging Syst. Technol*., 2020, **31**, 955–971. doi:10.1002/ima.22494.
19. Kirar, B.S.; Reddy, G. R. S. & Agrawal, D.K. Glaucoma detection using ss-qb-vmd-based fine sub-band images from fundus images. *IETE J. Research*., 2021, **69**, 4909–4920. doi:10.1080/03772063.2021.1959424.
20. Almeida-Galarraga, D.; Benavides-Montenegro, K.; Insuasti-Cruz, E.; Lovato-Villacis, N.; Suarez-Jaramillo, V.; Tene-Hurtado, D.; Tirado-Espin, A. & Villalba-Meneses, G.F. Glaucoma detection through digital processing from fundus images using MATLAB. *In* 2nd *Int. Conf. Inf. Syst. Software Technol. (ICI2ST)*, 2021. doi:10.1109/ici2st51859.2021.00014.
21. Devi, K.*„ et. al.* Texture Based Feature Extraction and Classification of Retinal Fundus Image for Glaucoma Detection. Proceedings of the 2nd International Conference on Smart Electronics and Communication (ICOSEC), 2021, pp. 1302–1307.
22. Manghnani, P. & Moghe, A. Glaucoma detection using bi-dimensional empirical mode decomposition from retinal fundus images. *Int. J. Intell. Eng. Syst*., 2021, **14**, 249–257. doi:10.22266/ijies2021.1231.23.
23. Devecioglu, O.C.; Malik, J.; Ince, T.; Kiranyaz, S.; Atalay, E. & Gabbouj, M. Real-time glaucoma detection from digital fundus images using self-onns. *IEEE Access*., 2021, **9**, 140031–140041. doi:10.1109/access.2021.3118102.
24. Singh, L.K.; Pooja, N.; Garg, H.; Khanna, M. & Bhadoria, R.S. An enhanced deep image model for glaucoma diagnosis using feature-based detection in retinal fundus. *Med. Biol. Eng. Comput*., 2021, **59**, 333–353. doi:10.1007/s11517-020-02307-5.
25. Sonti, K. & Dhuli, R. Shape and texture based identification of glaucoma from retinal fundus images. *Biomed. Signal Process. Control*., 2022, **73**, 103473. doi:10.1016/j.bspc.2021.103473.
26. David, D.S.; Selvi, S. a. M.; Sivaprakash, S.; Raja, P.V.; Sharma, D.K.; Dadheech, P. & Sengan, S. Enhanced detection of glaucoma on ensemble convolutional neural network for clinical informatics. *Comput. Mater. Contiua*., 2022, **70**(2), 2563–2579. doi:10.32604/cmc.2022.020059.
27. Chana, I. A cogitative analysis of load balancing technique with job migration in grid environment. World congr. Inf. Commun. Technol. (WICT), Mumbai, IEEE proc. Paper, 2011, 77-82. doi:10.1109/WICT.2011.6141221.
28. Pin, K.; Chang, J.H. & Nam, Y. Comparative study of transfer learning models for retinal disease diagnosis from fundus images. *Comput. Mater. Contiua.,* 2022, **70**(3), 5821–5834.

doi:10.32604/cmc.2022.021943.
29. Zuiderveld, K. Contrast limited adaptive histograph equalization. *In* Proc. of Graphic Gems IV, San Diego, Academic Press Professional., 1994, pp. 474–485.
30. Chana, I. Variable threshold-based hierarchical load balancing technique in Grid. *Eng. comput*., 2015, **31**, 597-615.
doi:10.1007/s00366-014-0364-z.
31. Nunes, J.C.; Guyot, S. & DeleChelle, E. Texture analysis based on local analysis of the bidimensional empirical mode decomposition. *Mach. Vis. Appl*., 2005, **16**, 177–188.
doi:10.1007/s00138-004-0170-5.
32. Dragomiretskiy, K. & Zosso, D. Two-Dimensional variational mode decomposition. *In Lect. Notes Comput. Sci.,* 2015, 197–208.
doi:10.1007/978-3-319-14612-6_15.
33. Agrawal, D.K.; Kirar, B.S. & Pachori, R.B. Automated glaucoma detection using quasi-bivariate variational mode decomposition from fundus images. *IET Image Process*., 2020, ***13***, 2401–2408.
doi:10.1049/iet-ipr.2019.0036.
34. Gonzalez, R.C. & Woods, R.E. *Digital Image Process*. 3rd ed. 2014.
35. Kononenko, I. Estimating attributes: analysis and extensions of relief. Lect. Notes Comput. Sci., 1994, 171–182.
doi:10.1007/3-540-57868-4_57.
36. Suykens, J.; Lukas, L.; Van Dooren, P. & Vandewalle, J. Least squares support vector machine classifiers. *Neural Process*., 1999, **9**, 293–300.
doi:10.1023/A:1018628609742.
37. Srinivas, B. & Rao, G.S. Segmentation of Multi-Modal MRI brain tumor sub-regions using deep learning. *J. Electr. Eng. Technol*., 2020, **15**, 1899–1909.
doi:10.1007/s42835-020-00448-z.
38. Yadav, A.K.; Pateriya, R.K.; Gupta, N.K.; Gupta, P.; Saini, D.K. & Alahmadi, M. Hybrid machine learning model for face recognition using SVM. *Comput. Mater. Contiua*, 2022, **72**, 2697–2712.
doi:10.32604/cmc.2022.023052.
39. Almalki, Y.E.; Shaf, A.; Ali, T.; Aamir, M.; Alduraibi, S.K.; Almutiri, S.M.; Irfan, M.; Basha, M.A.A.; Alduraibi, A.K.; Alamri, A.M.; Azam, M.Z.; Alshamrani, K. & Alshamrani, H.A. Breast cancer detection in Saudi Arabian women using hybrid machine learning on mammographic images. *Comput. Mater. Continua,* 2022, **72**, 4833–4851.
doi:10.32604/cmc.2022.027111.
40. Bhujade, R.K. & Asthana, S. An extensive comparative analysis on various efficient techniques for image Super-Resolution. *Int. J. Emerging Technol. Adv. Eng*., 2022, **12**, 153–158.
doi:10.46338/ijetae1122_16.
41. Guerroum, M.; Zegrari, M.; Masmoudi, M.; Berquedich, M. & Elmahjoub, A.A. Machine learning technics for remaining useful life prediction using diagnosis data: a case study of a jaw crusher. *Int. J. Emerging Technol. Adv. Eng*., 2022, **12**(10), 122–135.
doi:10.46338/ijetae1022_14.
42. Agustono, I.; Asrol, M.; Budiman, A.S.; Djuana, E. & Gunawan, F.E. State of charge prediction of lead acid battery using transformer neural network for solar smart dome 4.0. *Int. J. Emerging Technol. Adv. Eng*., 2022, **12**(10), 1–10.
doi:10.46338/ijetae1022_01.
43. Jain, N. & Singh, P. Binary pattern for copy-move image forgery detection. in handbook of machine vision and augmented intelligence. *In* Lect. Notes electr. Eng. 2023, **1007**.
doi:10.1007/978-981-99-0189-0_37.
44. Chana, I. Job migration policies for grid environment. *Wirel. Pers. Commun*., 2016, **89**, 241–269.
doi:10.1007/s11277-016-3264-2.
45. Apipawinwongsa, P. & Limpiyakorn, Y. Counterfeit luxury handbag materials image classification using deep learning and local binary pattern. *Int. J. Emerging Technol. Adv. Eng*., 2022, **12**, 41–48.
doi:10.46338/ijetae0922_05.
46. Wei, Y.; Machica, I.K.D.; Dumdumaya, C.E.; Arroyo, J.C.T. & Delima, A. P. Liveness detection based on improved convolutional neural network for face recognition security. *Int. J. Emerging Technol. Adv. Eng*., 2022, **12**, 45–53.
doi:10.46338/ijetae0822_06.
47. Clarin, J. A. Comparison of the performance of several regression algorithms in predicting the quality of white wine in WEKA. *Int. J. Emerging Technol. Adv. Eng*., 2022, **12**, 20–26.
doi:10.46338/ijetae0722_03.
48. Jain N. K. Image forgery detection using biorthogonal wavelet transform. *In* Conference on Machine Vision and Augmented Intelligence (MAI-2022), NIT Jamshedpur, 4-7 March 2022.
49. Abdelhafid, E.; Aymane, E.; Benayad, N.; Abdelalim, S.; Hachem, E.Y. a. M.; Rachid, O.H.T. & Brahim, B. ECG arrhythmia classification using convolutional neural Network. *Int. J. Emerging Technol. Adv. Eng*., 2022, **12**, 186–195.
doi:10.46338/ijetae0722_19.
50. Baharun, N.; Faezah, N.; Masrom, S.; Mohamad Yusri, N.A.; Abd Rahman, A.S. Auto modelling for machine learning: A comparison implementation between rapidminer and python. *Int. J. Emerging Technol. Adv. Eng*., 2022, **12**. 15-27.
doi:10.46338/ijetae0522_03.
51. Siguas, R.P.; Solis, H.M.; Solis, E.M.; Zamudio, L.M. & Artezano, A.R. application proposal for gastritis diagnosis and treatment applying machine learning. *Int. J. Emerging Technol. Adv. Eng*., 2022, **12**, 32–38.
doi:10.46338/ijetae0422_05.
52. Rathore,Neeraj. Report on hierarchical load balancing technique in grid environment. *i-manager's J. Inf. Technol*. 2013, **2**, 21-35.
doi:10.26634/jit.2.4.2541.
53. Dylan, C. & Rangkuti, A. H. WhatsApp Chatbot customer service using natural language processing and support vector machine. *Int. J. Emerging Technol. Adv. Eng*. 2022, **12**, 130–136.
doi:10.46338/ijetae0222_15.

54. Infusi, M.Z.; Kusuma, G.P. & Arham, D.A. Prediction of local government revenue using data mining method. *Int. J. Emerging Technol. Adv. Eng*. 2022, **12**, 63–74. doi:10.46338/ijetae0122_07.
55. Thakur, M.A. & Kumar, R. Optimizing smart manufacturing with iot integration and leveraging machine learning analysis. *Af. Diaspora J. Math. (Ugc Care Group I)*, *Neuro Quant*.. 2022 **20**, 1620-1629. doi: 10.48047/NQ.2022.20.18.NQ8817.
56. Jain N.K. Binary pattern for copy move image forgery detection. *In* International Conference on Machine Vision and Augmented Intelligence (MAI-2022), NIT Jamshedpur, 4-7 March. 2022.
57. Hasan, K.K.; Hairuddin, M.A.; Mustapa, R.F.; Nordin, S.A. & Ashar, N.D.K. Machine learning approach of optimal frequency tuning for capacitive wireless power transfer system. *Int. J. Emerging Technol. Adv. Eng*. 2022, **12**, 65-71. doi: 10.46338/ijetae1122_07.
58. Kumar, S. & Mishra, S.K. Survey on challenges and techniques for improving energy efficiency IOT network. *Int. J. Emerging Technol. Adv. Eng*. 2019, **9**, 151-155.
59. Agarwal, P.; Rawat, M. P. & Singh, N. Tackling Climate change with the help of Machine Learning. *Int. J. Emerging Technol. Adv. Eng*., 2019, **9**, 163-166.
60. Kumari, J. & Sarwagi, A. An efficient proposed approach to classify the breast cancer dataset using neural network. *Int. J. Emerging Technol. Adv. Eng*. 2019, **9**, 212-217.
61. Rathore, N. Dynamic threshold based load balancing algorithms. *Wireless Pers. Commun*. 2016, **91**, 151-185. doi: 10.1007/s11277-016-3452-0.
62. Agrawal, M.; Khan, A.U. & Shukla, P. Deep long short term memory model for stock price prediction using technical indicators. *Int. J. Emerging Technol. Adv. Eng*. 2019, **9**, 206-210.
63. Jain, N.K. & Mishra, A. An efficient image forgery detection using biorthogonal wavelet transform and improved relevance vector machine. *Wireless Pers. Commun.* 2018, **101**, 1983–2008. doi: 10.1007/s11277-018-5802-6.
64. Teja, U.H. & Choubey, S.B. Electronic nose - A big part of our future. *Int. J. Emerging Technol. Adv. Eng*. 2019, **9**, 93-97.
65. Tiwari, K.; Birthare, M. & Upadhyay, R. Proposal of smart mirror using raspberry PI. *Int. J. Emerging Technol. Adv. Eng*. 2019, **9**, 63-65.
66. Reddy, B.S.; Sathyanarayana, S.K. & Prasad, L.V.R.C. Robust wireless sensor network using cognitive radio. *Int. J. Emerging Technol. Adv. Eng*. 2019, **9**, 123-130.
67. Pande, S. & Purohit, A. Unveiling the impact of extreme learning machine in the defence and military. *Def. Sci. J*. 2024, **74,** 512-517.
68. Thakur, M.A. & Kumar, R. Review of smart manufacturing with IoT integration and leveraging machine learning analysis. *Af. Diaspora J. Math*. 2022, **25**, 88-101.
69. Rathore, N. & Chana, I. Load balancing and job migration techniques in grid: A survey of recent trends. *Wireless Pers. Commun*. **79**, 2089-2125. doi:10.1007/s11277-014-1975-9.
70. Sharma, V. & Kumar, R. Topological broadcasting using parameter sensitivity based logical proximity graphs in coordinated ground-flying Ad Hoc networks. *J. Wirel. Mob. Netw. Ubiquitous Comput*. 2015, **6**, 54-72. doi:10.22667/JOWUA.2015.09.31.054.
71. Bouris, E.; Odugbo, O.P.; Rasheed, H.; Jin, S.; Fei, Z.; Morales, E. & Caprioli, J. A neural network for the detection of glaucoma from optic disc photographs. *Investigative Ophthalmol. & Visual Sci.*, 2024, **65**, 1634.
72. Wiharto, Harjoko, W.T. & Suryani, E. e-LSTM: Efficient net and long short-term memory model for detection of glaucoma diseases. *Int. J. Online Biomed. Eng.,* 2024, **20**, 64. doi: 10.3991/ijoe.v20i10.48603
73. Manghnani, P. & Moghe. A.A. BDIMFs based features fusion and classification for glaucoma prediction. *In* 2024 IEEE International Students' Conference on Electrical, Electronics and Computer Science (SCEECS), Bhopal, India, 2024, pp. 1-6, doi: 10.1109/SCEECS61402.2024.10481851

CONTRIBUTORS

Ms Pooja Manghnani obtainer MTech in Information Technology from RGPV, Bhopal. She is presently working in Govt. Women's Polytechnic College Bhopal as HOD Computer Science Department. Her research interests include: Image processing.
In the current study, she contributed to conception and design, data collection, analysis and interpretation of results.

Dr Asmita A. Moghe obtained PhD Maulana Azad National Institute of Technology Bhopal. She is presently working in University Institute of Technology, RGPV, Bhopal as HOD Information Technology Department. Her research interests include: Image processing.
In the current study she contributed to analysed results, drafted manuscript, reviewed the manuscript.